Science in China Series E: Technological Sciences

Nano-scaled iron-carbon precipitates in HSLC and HSLA steels

FU Jie[1], WU HuaJie[1†], LIU YangChun[1] & KANG YongLin[2]

[1] School of Metallurgical and Ecological Engineering, University of Science and Technology Beijing, Beijing 100083, China;
[2] School of Materials Science and Engineering, University of Science and Technology Beijing, Beijing 100083, China

This paper studies the composition, quantity and particle size distribution of nano-scaled precipitates with size less than 20 nm in high strength low carbon (HSLC) steel and their effects on mechanical properties of HSLC steel by means of mass balance calculation of nano-scaled precipitates measured by chemical phase analysis plus SAXS method, high-resolution TEM analysis and thermodynamics calculation, as well as temper rapid cooling treatment of ZJ330. It is found that there existed a large quantity of nano-scaled iron-carbon precipitates with size less than 18 nm in low carbon steel produced by CSP and they are mainly Fe-O-C and Fe-Ti-O-C precipitates formed below temperature A_1. These precipitates have obvious precipitation strengthening effect on HSLC steel and this may be regarded as one of the main reasons why HSLC steel has higher strength. There also existed a lot of iron-carbon precipitates with size less than 36 nm in HSLA steels.

HSLC steel, high strength low alloyed steel (HSLA steel), iron-carbon precipitates, precipitation strengthening

Low carbon steels, with carbon content ranging from <0.06% to 0.25% (including Q195, Q235 or SS-330, SS-400, etc.) and generally with a yield strength (σ_s) about 200 MPa when produced by traditional processes, are used extensively. To greatly increase the yield strength of the low carbon steel, or even to double it to 400 MPa, is one of the main goals in steel research around the world. Such a goal is exactly in accordance with the demands of sustainable development and has strategic significance in the steel industry.

TSCR is one of the techniques to produce "New Generation of Steel". Such products are mainly high strength low alloyed (HSLA) steels alloyed with vanadium or niobium developed overseas[1,2].

So far, Guangzhou Zhujiang Iron and Steel Co. Ltd, in cooperation with University of Science

Received December 15, 2005; accepted October 13, 2006
doi: 10.1007/s11431-007-0008-2
†Corresponding author (email: whjyeah@163.com)
Supported by the National Natural Science Foundation of China (Grant No. 50334010), the State Foundation for Key Projects: New Generation of Steels (Grant No. G1998061500)

and Technology Beijing, is the first plant that has developed and produce in bulk high strength low carbon (HSLC) steel through EAF-CSP technique. Though without micro-alloy elements additions, the yield strength of HSLC steel thus achieved is equivalent to that of HSLA steel with Nb or V addition with σ_s around 345－410 MPa[3].

In previous researches on the reason why HSLC steels produced by CSP process have high strength, the authors found that there existed a large number of nano-scaled oxides and sulfides with particle size about several tens of nm to several hundreds of nm, and there also existed a large number of nano-scaled precipitating particles with a size less than 20 nm which have spinel structure[4]. Nano-scaled AlN particles were also observed and their precipitation dynamics was discussed[5]. Through studying the effect of nano-scaled iron carbides on the mechanical properties of steels produced by CSP process, we pointed out that there existed a great number of nano-scaled precipitates with sizes less than 18 nm, mainly iron carbides, in slabs, rolling pieces and plates[6, 7].

The quantitative ties are still uncertain on the part of various elements. There exist some arguments about precipitation strengthening, including that of nano-scaled precipitates. Ref. [8] indicated that the nano-scaled precipitates in ZJ330 and Q195 steels with sizes less than 20 nm were nano-scaled oxides with spinel structure.

In this paper, the types of precipitates with sizes less than 20 nm and their effects on mechanical properties, as well as the precipitation strengthening effect on HSLC steel and HSLA steel, are studied.

1 Chemical phase analyses of nano-scaled precipitates, their small angle X-ray scattering and mass balance calculation

It is difficult to ascertain the volume fraction of nano-scaled precipitates metallographically, while chemical phase analysis (electrolytic dissolution technology) plus SAXS is effective in identifying the composition, mass or volume percentage of the nano-scaled precipitate particles with different types and sizes.

The chemical phase analysis process of low carbon steel we used is as follows:

1) The steel samples were polished and electrolyzed, and then powder precipitates consisting of M_3C (cementite and iron carbon precipitates), $M(C_xN_y)$, sulfides, AlN and oxides were obtained.

2) $M(C_xN_y)$ and oxides were obtained when the iron carbide, sulfide and AlN had been removed from the electrolysis powder.

3) Then the stable oxides were obtained by electrolytic dissolution technique.

Because the $M(C_xN_y)$ and the oxide were very small in quantity, M_3C is represented by the overall quantity of the electrolysis powder in this paper.

The particle size distribution of the powder was measured by means of SAXS with X-ray diffracto-spectrometer and Kratky small angle scattering goniomter according to GB/T 13221-91 (ISO/TS 13762-2001) specification with error smaller than 10%. Analysis and testing work were carried out in the Chinese Iron and Steel Materials Testing Centre. The chemical composition is shown in Table 1, in which the hot rolled plates, the slab and the rolling piece are not derived from the same heat.

Table 1 Chemical composition (wt%) of testing steels

Testing materials	C	Si	Mn	S	P	Cu	Alt	Als	N	T.O
ZJ330 hot rolled plates	0.060	0.11	0.28	0.006	0.012	0.12	0.020	0.016	0.0044	0.0028
ZJ330 slab	0.051	0.04	0.39	0.012	0.015	0.16	0.031	0.0306	0.0044	0.0030
ZJ330 rolling piece	0.051	0.04	0.39	0.012	0.015	0.16	0.031	0.0306	0.0044	0.0030
ZJ510 hot rolled plates[a)]	0.18	0.28	1.21	0.004	0.023	0.11	0.024	0.021	0.0034	0.0024

a) The ZJ510 steel sample contained 0.005%Ti, which was in the raw material but not added intentionally.

X-ray analyses of the electrolysis powder showed that there existed M_3C phase in the slabs, rolling pieces and hot strips. Their composition and mass percentage are listed in Table 2. ZJ510 steel contained a certain $M(C_xN_y)$ phase, with 0.0044% Ti, and the overall quantity was 0.0062%, so the mass percentage of those with size less than 18 nm were ignored.

The combined nitrogen and sulfur contents in the testing materials are shown in Table 3 and the oxide inclusions in ZJ330 are shown in Table 4.

Table 2 Mass percentage of $M_3(C_xN_y)$ phase,%

Testing materials	Chemical composition (mass%) of $M_3(C_xN_y)$					
	Fe	Mn	Ni	C	N	Σ
ZJ330 hot rolled plates	0.823	0.004	0.001	0.059	0.001	0.888
ZJ330 slabs	0.688	0.008	0.002	0.050	0.001	0.749
ZJ330 rolling piece of the first pass	0.694	0.008	0.002	0.050	0.001	0.755
ZJ330 rolling piece of the second pass	0.724	0.009	0.002	0.052	0.001	0.788
ZJ510 hot rolled plates	2.054	0.067	0.002	0.151	0.002	2.278

Table 3 Combined nitrogen and sulfur contents in experimental steels, wt%

Testing materials	AlN	Combined nitrogen	Combined sulfur
ZJ330 hot rolled plates	0.0020	0.0018	0.0058
ZJ330 slabs	0.0023	0.0020	0.0116
ZJ330 rolling piece of the first pass	0.0023	0.0020	0.0116
ZJ330 rolling piece of the second pass	0.0023	0.0020	0.0116
ZJ510 hot rolled plates	0.0021	0.0038	0.0039

Table 4 Quantitative analysis of oxide inclusions, wt%

Al_2O_3	SiO_2	CaO	FeO	MgO	TiO_2	MnO_2	NiO	Cr_2O_3	Σ
0.00178	0.00257	0.00096	0.00066	0.00030	0.00002	0.00003	0.00001	0.00003	0.00636

Note: the total oxygen content in the steel is 0.0030%

The particle size distribution of electrolysis powder and mass percentage of particles smaller than 18 nm is shown in Figure 1 and Table 5. The $f(D)$ in histogram is the particle size distribution frequency that shows the average mass percentage of 1 nm range particles in different particle size ranges. For example, at $f(D) = 0.3\%/\text{nm}$, the mass percentage of 1－5 nm range particles is 0.3%/nm×(5－1) nm=1.2%. In Figure 1, there are two peak values in histogram that maybe relate to two kinds of size distribution of different particles. Their precipitation mechanism is still under investigation.

The particles with a size less than 18 nm from the electrolysis powder calculated by means of chemical phase analysis plus small angle X-ray scattering (SAXS) method were iron carbides, alloy carbides, sulfides, AlN and oxides, as mentioned above.

For particles with a size less than 18 nm, according to the law of mass conservation, we have

$$W_{\text{powder}} = W_{\text{iron carbide}} + W_{\text{alloy carbide}} + W_{\text{sulfide}} + W_{\text{AlN}} + W_{\text{oxide}},$$

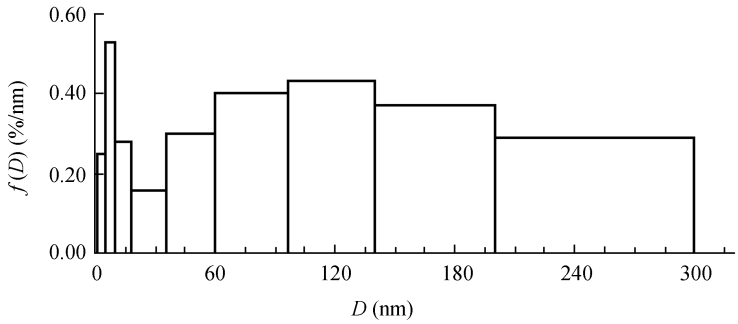

Figure 1 Histogram of particle size distribution of electrolysis powder of ZJ330 hot rolled plates.

Table 5 Mass percentage of particles with size less than 18 nm, wt%

Testing materials	The amount of electrolysis powder (wt%)	Percentage of different size particles in specimen (%)[a)]				<18 nm particles (wt%)
		1－5 nm	5－10 nm	10－18 nm	<18 nm	
ZJ330 hot rolled Plates	0.888	0.25/1.0	0.53/2.7	0.28/2.2	—/5.9	0.052
ZJ330 slabs	0.749	0.30/1.2	0.65/3.7	0.47/3.7	—/8.2	0.061
ZJ330 rolling piece of the first pass	0.755	0.47/1.9	0.99/4.9	0.82/6.6	—/13.4	0.101
ZJ330 rolling piece of the second pass	0.788	0.49/2.0	1.00/5.0	0.39/3.1	—/10.1	0.080
ZJ510 hot rolled plates	2.2783	0.21/0.8	0.46/2.3	0.11/0.9	—/4.0	0.091

a) Numerator: $f(D)$, %/nm; denominator: the ratio of mass percentage of different size particles to that of total particles.

where W_{powder} is the total mass percentage of all the precipitates with sizes less than 18 nm in the electrolysis powder, while $W_{\text{iron carbide}}$, $W_{\text{alloy carbide}}$, W_{sulfide}, W_{AlN} and W_{oxide} are the mass percentages of various precipitates with sizes less than 18 nm in the electrolysis powder, respectively. For hot rolled plate of ZJ330 steel, substituting the testing data in the above formula, we have

$$0.052 = W_{\text{iron carbide}} + 0 + (<<0.016) + (<0.0020) + (<<0.0064),$$

$$W_{\text{iron carbide}} = 0.052 - (<<0.0244) = (>>0.0276).$$

For hot rolled plates of ZJ510 steel, we have

$$0.091 = W_{\text{iron carbide}} + (<0.0062) + (<<0.0106) + (<0.0021) + (<<0.0064),$$

$$W_{\text{iron carbide}} = 0.091 - (<<0.0253) = (>>0.0657),$$

where << means far smaller, >> means far larger.

From Figure 1, we may derive a conclusion that the particles with sizes less than 18 nm are mainly iron-carbon precipitates. In regard to the calculation above, the quantity of oxides in ZJ510 steel is cited from the data of ZJ330 steel. The sulfide, oxide and AlN particles with sizes less than 18 nm in HSLC steels may have precipitation strengthening effect, according to the above analysis and the mass balance calculation, nevertheless, a supposition can be made that the nano-scaled iron carbon precipitates may have significant precipitation strengthening effect on HSLC steels.

2 HRTEM analysis results and thermodynamic calculation

It is difficult to identify the type, size and distribution of the particles less than 20 nm, especially those only several nm. In order to ascertain the type and precipitate mechanism, the electrolyzed powder particles were examined and analyzed by HRTEM.

The hot rolled carbon steel plate was electrolyzed for 24 h in an organic liquid, and then the extracted powder particles were placed in anhydrous alcohol and suspended by supersonic vibration. Then drops from the upper layer containing the nano-scaled powder particles were placed on a collodium film supported by a copper micromesh for drying. The samples were examined under a HRTEM JEM-2010 electron microscope and their chemical composition was analyzed by means of X-ray energy spectrum. The testing results are shown in Figures 2－5.

Figures 2－5 show that there existed three kinds of nano-scaled precipitates less than 20 nm in size in HSLC steels produced by CSP process, among which the first is the nano-scaled Fe-O-C precipitate (Figures 2 and 3). A large numbers of these particles were found in many regions and a clear carbon peak could be seen on the energy spectrum. Clustered nano-scaled precipitate particles about 5 nm were also observed by HRTEM. The energy spectrum (Figure 2(b)) was taken from a larger particle (about 10 nm) in the center, perhaps the same kind of Fe-O-C precipitate. The second one in Figure 4 is nano-scaled Fe-O precipitate with an oxygen peak but with no carbon peak. A nano-scaled Fe-Ti-O-C precipitate is shown in Figure 5, whose size is more than 20 nm. Because of the presence of nano-scaled iron-oxygen precipitates, it can be concluded that the carbon peak of energy spectrum of the other two kinds of precipitates were not introduced from collodium film.

It can be seen from the iron-carbon phase diagram that the equilibrium carbon content will decrease from about 0.022% to 0% when the temperature decreases from A_1 to room temperature.

According to thermodynamic data in refs. [9,10], the following calculations can be made:

$$\mathrm{Fe_{0.947}O_{(l)}=Fe_{0.947}O(s)}, \tag{1}$$

$$\Delta G_1^{\,0}=-31338.16+18.99T.$$

The transition temperature is 1377℃.

Under this transition temperature we can deduce

$$\mathrm{Fe_{(l)}+1/2O_{2(g)}=FeO_{(l)}} \qquad \Delta G^0=-256060.8+53.68T \quad \mathrm{J/mol}$$

$$\mathrm{1/2O_{2(g)}=[O]} \qquad \Delta G^0=-117110-3.39T \quad \mathrm{J/mol}$$

$$\mathrm{Fe_{(l)}=Fe(s)} \qquad \Delta G^0=-13807.2+7.61T \quad \mathrm{J/mol}$$

$$\mathrm{FeO_{(l)}=FeO(s)} \qquad \Delta G^0=-31338.16+18.99T \quad \mathrm{J/mol}$$

$$\mathrm{Fe_{(s)}+[O]=FeO(s)} \tag{2}$$

$$\Delta G_2^{\,0}=-156481.95+68.45T \quad \mathrm{J/mol}$$

$$\mathrm{2Fe_{(s)}+3/2O_{2(g)}=Fe_2O_{3(s)}} \qquad \Delta G^0=-814122.72+250.66T \quad \mathrm{J/mol}$$

$$\mathrm{3/2O_{2(g)}=3[O]} \qquad \Delta G^0=-351330-10.17T \quad \mathrm{J/mol}$$

$$\mathrm{2Fe_{(s)}+3[O]=Fe_2O_{3(s)}} \tag{3}$$

$$\Delta G_3^{\,0}=-462792.72+260.83T \quad \mathrm{J/mol}$$

$$\mathrm{3\,Fe_{(s)}+2O_{2(g)}=Fe_3O_{4(s)}} \qquad \Delta G^0=-1102191+307.36T \quad \mathrm{J/mol}$$

$$\mathrm{2O_{2(g)}=4[O]} \qquad \Delta G^0=-468440-13.56T \quad \mathrm{J/mol}$$

$$\mathrm{3\,Fe_{(s)}+4[O]=Fe_3O_4(s)} \tag{4}$$

$$\Delta G_4^{\,0}=-633751+320.92T \quad \mathrm{J/mol}$$

By eqs. (1)－(4) the relationship between standard free energy and temperature of different iron-oxides can be obtained (Figure 6).

Figure 6 shows that Fe_3O_4 is apt to precipitate below 1377℃, so we may conclude that the nano-scaled iron-oxygen precipitates with sizes less than 18 nm founded in HSLC steels should be Fe_3O_4.

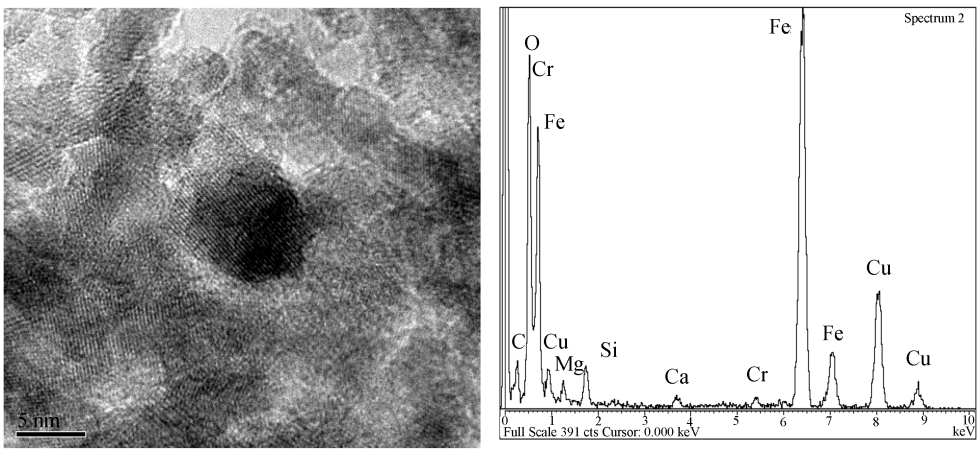

(a) (b)

Figure 2 HRTEM image of nano-scaled Fe-O-C precipitates from the electrolysis powder of ZJ330 steel (a) and its energy spectrum (b).

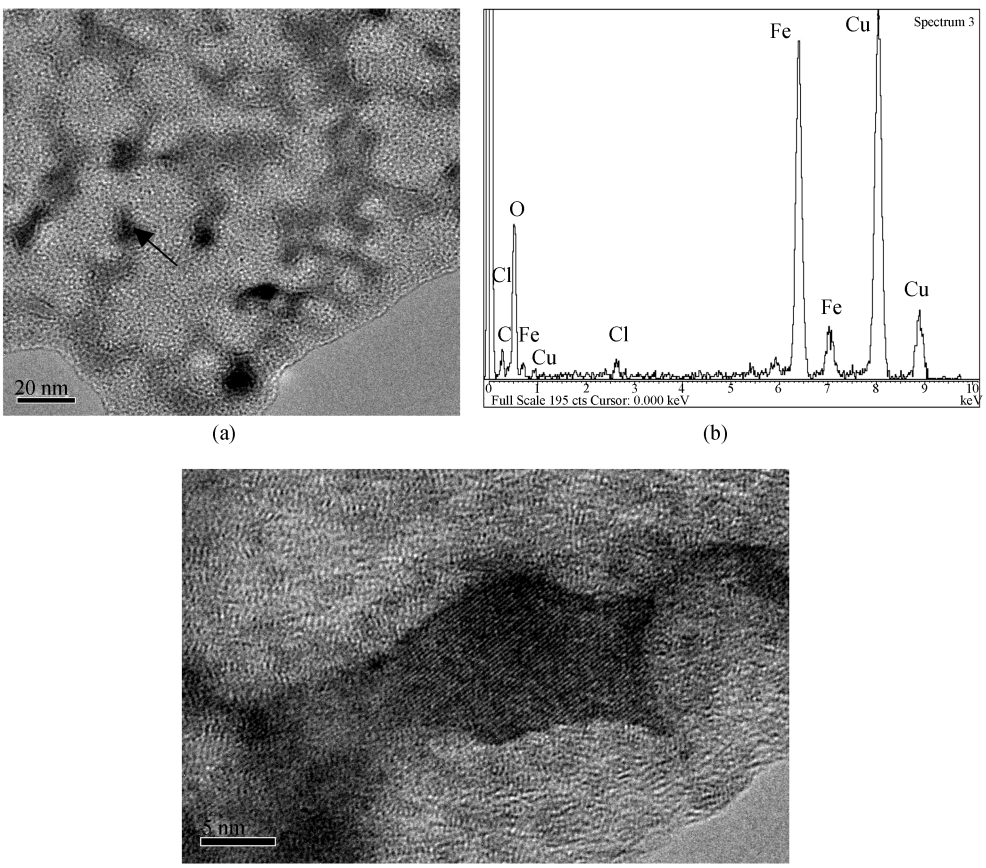

(a) (b)

(c)

Figure 3 HRTEM image of nano-scaled Fe-O-C precipitate from the electrolysis powder of ZJ510 steel (a), the energy spectrum (b) and HRTEM image of the arrow particle in (a) with greater multiple (c).

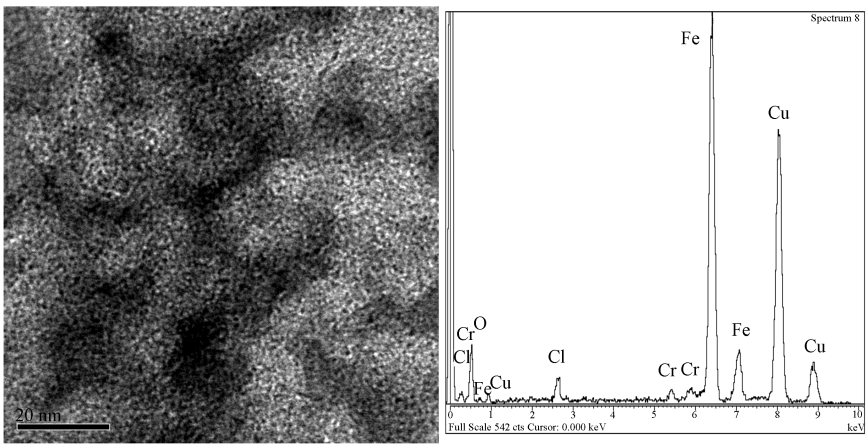

(a) (b)

Figure 4 HRTEM image of nano-scaled Fe-O precipitate from the electrolysis powder of ZJ510 steel (a) and its energy spectrum (b).

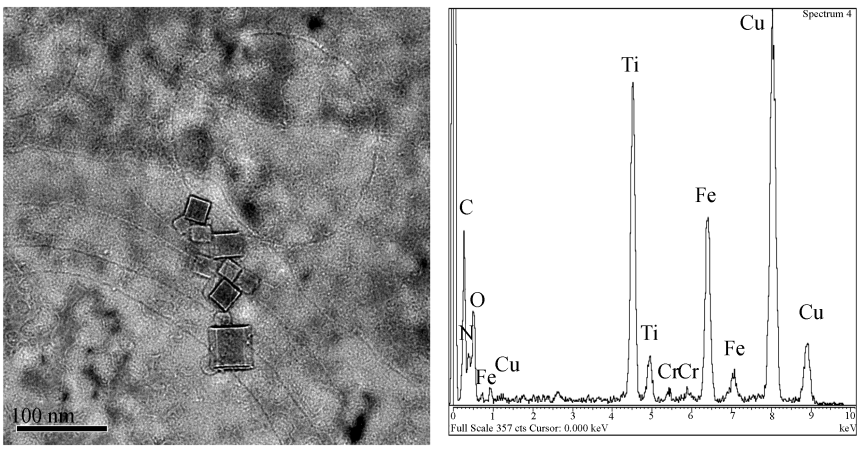

(a) (b)

Figure 5 HRTEM image of some nano-scaled precipitate with chemical composition Fe, Ti, O, C from the electrolysis powder of ZJ510 steel (a) and its energy spectrum (b).

The precipitation temperature of Fe_3O_4 can be expressed by

$$\Delta G_4^0 = -RT\ln K = -RT\ln\frac{a_{Fe_3O_4}}{a_{Fe}^3 a_O^4}. \quad (5)$$

For low carbon steel, the activity of Fe_3O_4 and Fe is considered as 1 and the activity of oxygen is represented by concentration, so we have

$$\lg[O] = -\frac{8274.75}{T} + 4.19. \quad (6)$$

Assuming the soluble oxygen content in steels assumed to be 2 ppm, the beginning precipitation temperature of Fe_3O_4 is 776℃.

The discussion above suggests that the nano-scaled Fe-O-C precipitates with sizes less than 18 nm probably nucleate on Fe-O precipitates (Fe_3O_4) in a heterogeneous nucleating manner.

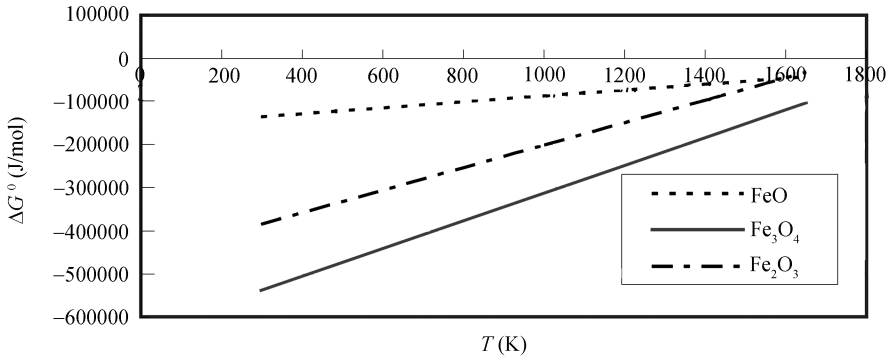

Figure 6 Relationship between standard free energy and temperature of various iron-oxides.

3 The control of nano-scaled precipitates in HSLC steels—temper-rapid cooling process

In order to study the precipitation temperature, nucleating, growing, coarsening and strengthening effects of the nano-scaled iron-carbon precipitates less than 18 nm in size, three groups of special tests were carried out. Group one was to study the effect of heat treatment temperature below A_1 on mechanical properties, and the test was repeated (shown as mechanical properties 2). The second was to investigate the effect of holding time on mechanical properties, in which HSLC steel ZJ330 (coiling No. 53921) was used. The experimental results are shown in Table 6 and Figure 7. The third was to test the reproducibility of the second, in which the material was also ZJ330 (coiling No. 53931) and σ_s, σ_b, δ were 351 MPa，425 MPa and 42%, respectively. The experimental results are shown in Figure 8.

Table 6 The effect of temper temperature and cooling method on mechanical properties of ZJ330[a)]

Serial number	Temper temperature(℃)	Cooling method	Yield strength 1 (MPa)	Tensile strength 1 (MPa)	Elongation 1 (%)	Yield strength 2 (MPa)	Tensile strength 2 (MPa)	Elongation 2(%)
1	Original sample		339	397	45	344	408	39
2	200	water cooling	341	399	48	336	406	44
3	300	water cooling	330	405	45	339	414	46
4	400	water cooling	335	410	40	330	407	43
5	500	water cooling	351	413	43	342	420	41
61	600	water cooling	403	480	30	410	490	29
62	600	air cooling	329	403	41	345	405	41
63	600	furnace cooling	320	397	43	322	397	43
7	700	water cooling	468	651	13	458	625	16

a) Holding time: 20 min.

The yield strength increased to 410 MPa (increased by 70 MPa) while the elongation was about 30% for coiling No. 53921 when the sample was processed by temper-rapid cooling at 600℃. Similarly, the yield strength increased to 450 MPa (increased by 100 MPa) while the elongation was 22% for coiling No. 53931 when the sample was processed by temper-rapid cooling at 600℃. The yield strength increased more while the elongation decreased at 700℃.

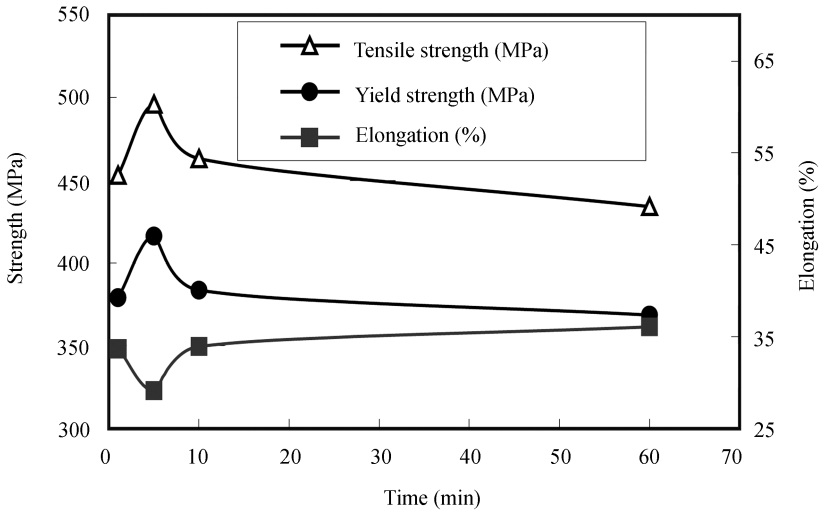

Figure 7 Effect of holding time at 600℃ on mechanical properties.

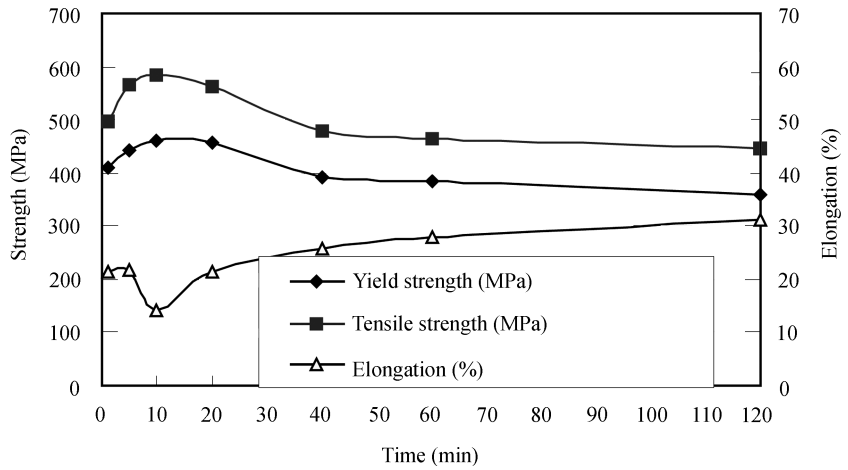

Figure 8 Effect of holding time at 600℃ on mechanical properties.

With these experimental results, we can explain why HSLC steels have higher strength. The iron-carbon precipitates that originally existed in steels were dissolved when the samples were held at 600℃ for a period of time. When they were cooled down again at a speed faster than that during CSP process, the size of the nano iron-carbon precipitate newly formed was smaller and had an enhanced strength; when the samples were held at 600℃ for a longer period, the nano-scaled iron-carbon precipitate formed above 600℃ would be coarsened and their strength decreased.

No prior phase transformation will take place below A_1 temperature. The grain size remains 8 μm during the temper-rapid cooling (Figure 9), but σ_s is greatly increased. It can be concluded therefore that the strength increase results from the effect of nano-scaled iron-carbon precipitation rather than that of phase transformation and grain refining.

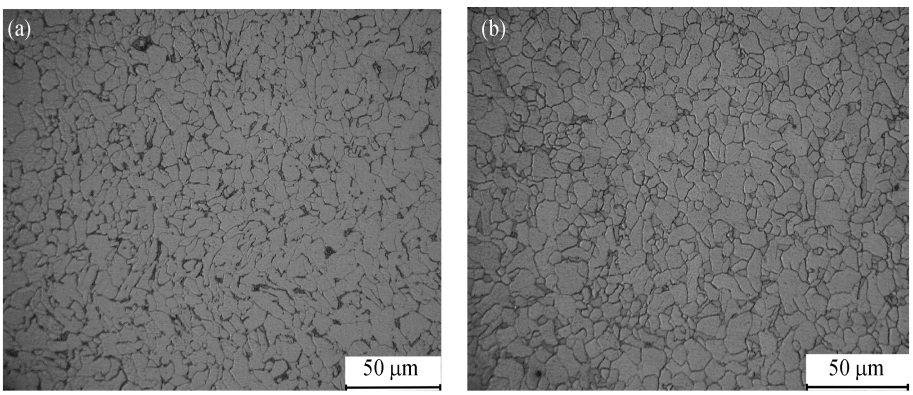

Figure 9 The microstructure of ZJ330 steel before (a) and after (b) tempering at 700℃.

According to the binary alloy Fe-Cu phase diagrams[11], it is possible to precipitate ε-Cu at a lower temperature. But obvious aging strengthening effect can only be obtained when Cu content is higher than 0.5% (normally 1%—3%) at 600℃[12,13]. The Cu content in ZJ330 is only 0.12% which is smaller than the equilibrium solid solubility of Cu in iron at 600℃. Therefore, no aging strengthening effect of Cu would happen there during tempering at 600℃ and the aging strengthening should be attributed to the precipitation of iron carbon precipitate. In the production practice of Zhujiang Company, the yield strength would change little when Cu content was from <0.1% to 0.3%. Sometimes, the yield strength of steel bearing higher Cu was lower than that of steel bearing lower Cu. This fact suggests that no obvious precipitation of ε-Cu happened under the conditions of CSP.

4 Nano-scaled iron carbon precipitates in HSLA steel

HSLA steels samples B2C (HSLA steels, σ_s about 800 MPa)[14] and 70A (Corten 700, Ti 0.125%) have been analyzed by means of chemical phase analysis plus SAXS method, and the mass percentage of electrolyzed powder and M(C_XN_Y) with sizes less than 36 nm are shown in Tables 7 and 8.

Table 7 Mass percentage of M(C_XN_Y) particle with different sizes in B2C sample

Species of particle	The amount of electrolysis powder (wt%)	Percentage of different sized particle in specimen (%)[a)]				Particle <18 nm (wt%)	Particle <36 nm (wt%)
		1—5 nm	5—10 nm	10—18 nm	18—36 nm		
Electrolysis powder,	0.4865	0.06/0.2	0.19/1.0	0.23/1.8	1.46/26.3	0.0146	0.1425
M (C_XN_Y)	0.0575	0.30/1.2	0.65/2.2	0.23/1.8	0.47/8.4	0.0036	0.0084

a) Numerator: $f(D)$, %/nm; denominator: the ratio of mass percentage of different size particles to that of total particles.

Tables 7 and 8 show that the mass percentage of M(C_XN_Y) particle with sizes less than 36 nm in B2C sample is much less than that of iron-carbon precipitate, and the mass percentage of M(C_XN_Y) particle with sizes less than 36 nm in 70A sample is equal to that of iron-carbon precipitate, so we should not ignore the contribution of nano-scaled iron carbon precipitate when studying the grain refining strengthening and precipitation strengthening of HSLA steels.

Table 8 Mass percentage of M(C_XN_Y) particle with different sizes in 70A sample

Species of particle	The amount of electrolysis powder (wt%)	Percentage of different sized particle in specimen (%)[a)]				Particle <18 nm (wt%)	Particle <36 nm (wt%)
		1－5 nm	5－10 nm	10－18 nm	18－36 nm		
Electrolysis powder,	0.3109	0.77/3.1	1.59/8.0	0.68/5.4	0.93/16.8	0.0513	0.1035
M (C_XN_Y)	0.0895	1.05/4.2	2.15/10.7	1.26/10.1	0.91/16.4	0.0224	0.0371

a) Numerator: $f(D)$, %/nm; denominator: the ratio of mass percentage of different size particles to that of total particles.

5 Conclusions

(1) The nano-scaled iron-carbon precipitate plays the main role in precipitation strengthening among the particles with sizes less than 20 nm in HSLC steels produced by CSP process, but the precipitation process, their nucleation and the particle structure await further studies.

(2) The yield strength of ZJ330 can be greatly increased to exceed 410 MPa and a better elongation can be achieved (about 30%) during the temper-rapid cooling process about 600℃ and with a holding time of 1－20 min.

(3) Under temper-rapid cooling conditions, no grain refinement will happen, so the strength increase is mainly due to the effect of the nano-scaled iron carbon precipitate.

(4) The control of the behavior of iron-carbon precipitates for TMCP process is an important factor during the continuous rolling process of low carbon steel.

(5) There exist a large quantity of nano-scaled iron carbon precipitates with sizes less than 36 nm in HSLA steels, the effect of which in HSLA steels are yet to be further studied.

We thank senior member of Chinese Academy of Science T. Ko for his supervision, encouragement and support. Thanks are also extended to Professor Fang Keming for his helps in preparation of the electrolytic powder samples for HRTEM analysis.

1 Li Y, Wilson J A, Crowther D N, et al. The effects of vanadium (Nb,Ti) on the microstructure and mechanical properties of thin slab cast steels. In: The Chinese Society for Metals, eds. TSCR'2002, Guangzhou, China, 2002, 218－234
2 Garcia C I, Tokarz C, Graham C, et al. Niobium HSLA steels producing the thin slab casting process: Hot strip mill products, properties and applications. In: The Chinese Society for Metals, eds. TSCR'2002, Guangzhou, China, 2002, 194－198
3 Fu J, Wang Z B, Kang Y L, et al. Research and development of HSLC steels produced by EAF-CSP technology. J Univ Sci Tech Beijing (in Chinese), 2003, 25(5): 449－454
4 Liu D L, Fu J, Kang Y L, et al. Oxide and sulfide dispersive precipitation and effects on microstructure and properties of low carbon steels. J Mater Sci Tech, 2002, 18(1): 7－9
5 Kang Y L, Yu H, Fu J, et al. Morphology and precipitation kinetics of AlN in hot strip of low carbon steel produced by compact strip production. Mater Sci Eng A, 2003, 351(1-2): 265－271
6 Fu J. New generation low carbon steel-HSLC steel. The Chinese Journal of Nonferrous Metals (in Chinese), 2004, 14(suppl.1): 82－90
7 Fu J, Kang Y L, Liu D L, et al. Nano-scale carbide and strengthening effect in low carbon steel produced by CSP process. J Univ Sci Tech Beijing (in Chinese), 2003, 25(4): 328－331
8 Weng Y Q, et al. Ultra Fine Grain Steel—The Theory and Control Technology of Structure Refinement of Steels (in Chinese). Beijing: Metallurgical Industry Press, 2003. 979
9 Turkdogan E T. Physical Chemistry of High Temperature Technology (in Chinese). Wei J H, Fu J trans. Beijing: Metallurgical Industry Press, 1988
10 Barin I. Thermochemical Data of Pure Substances (in Chinese). Cheng N L, Niu S T, Xu G Y et al. trans. Beijing: Science Press, 2003
11 Massalski T B. Binary alloy phase diagrams. ASM international®, 1996
12 Mao W M, Ren H P. Investigation of new structural steel strengthened by Cu precipitation (in Chinese). Transactions of Metal Heat Treatment, 1999, 20(1): 1－5
13 Mao W M, Ren H P. Development of structural steels containing copping. Iron and Steel (in Chinese), 2000, 35(6): 49－53
14 Liu D L, Kang Y L, Fu J, et al. Study of microstructure and mechanical properties of clean microalloyed steels. In: Liu G Q, Wang F M, Wang Z B, et al. eds. HSLA Steels'2000, Beijing: Metallurgical Industry Press, 2000. 267－271